ChemComm

Cite this: *Chem. Commun.*, 2012, **48**, 5668–5670

www.rsc.org/chemcomm

COMMUNICATION

Novel dithieno-benzo-imidazole-based Pb^{2+} sensors: substituent effects on sensitivity and reversibility†

Rudrakanta Satapathy, Yen-Hsing Wu and Hong-Cheu Lin*

Received 15th February 2012, Accepted 13th April 2012
DOI: 10.1039/c2cc31131c

Two novel dithieno-benzo-imidazole-based compounds (M2 and A2) showed remarkable sensitivities towards Pb^{2+} by 12-fold enhancement and 10-fold decay of fluorescence, respectively, in aqueous solutions. Substituent effects of different dithieno-benzo-imidazole-based moieties (M1, M2, A1 and A2) on the quantum yields, fluorescence lifetimes and sensitivities to Pb^{2+} along with the reversibilities by S^{2-} were investigated.

Owing to the biological, medicinal, oceanographic and environmental toxicity of cations, numerous analytical methods, such as neutron activation analysis, ion sensitivity (to electrodes), flame photometry, atomic absorption spectrometry, electron microprobe analysis and inductively coupled plasma-mass spectroscopy, were developed for their detection.[1] However, due to the drawbacks such as expensiveness, time consumption, difficulties in continuous monitoring and requirement of large size samples in these detection methods, the methods based on fluorescent sensors are preferable as they offer diverse advantages in terms of sensitivity, selectivity, response time and local observation (*e.g.*, fluorescence imaging spectroscopy).[2] Lead, being a poisonous neurotoxin substance, damages the nervous system. Excessive lead also causes cardiovascular, reproductive and developmental disorders in mammals and brain disorder.[3] Thus, development of selective and sensitive methods for the detection of lead ions is extensively challenging for chemists. For instance, fluorescence turn-on sensing mechanisms could be explained in terms of intramolecular charge transfer (ICT)[2] and/or chelation[5] effects, and the aggregation induced by quenchers is one of the rudimentary reasons for fluorescence turn-off.[5]

Recently several probes such as cyclen,[4a] imidazoquinoxaline,[4b] imidazopyrene,[4c] imidazophenazine,[4d] rhodamine[4e] and calixarene[4f] have been successfully reported for selective sensing of Pb^{2+}. To the best of our knowledge, thieno-imidazole-based sensors have not been reported so far. Therefore, two novel dithieno-benzo-imidazole-based compounds **M2** and **A2** were synthesized to find the effects of chelation by 'N' and 'S' linkages on selectivity and sensitivity towards target metal ions.

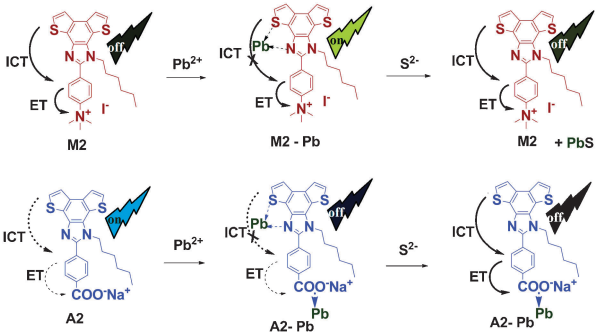

Fig. 1 Schematic representation of the fluorescence off–on–off and on–off–off mechanisms of **M2** and **A2**, respectively, towards Pb^{2+} and S^{2-}.

Fig. 1 shows the fluorescence off–on–off and on–off–off mechanisms for **M2** and **A2**, respectively, towards Pb^{2+} and S^{2-}.

Synthetic procedures for **M1**, **M2**, **A1** and **A2** are depicted in Scheme 1. The easiest way to prepare 3,3′-bithiophene was from 3-bromothiophene by treating with *n*-BuLi and Cu powder. 3,3′-Bithiophene was acylated by oxalic acid without the aid of any Lewis acid to yield compound **3**, which was coupled with 4-nitrobenzaldehyde in the presence of ammonium acetate in acetic acid to get compound **4**. *N*-Alkylation of compound **4** produced compound **5**. **M1** was prepared by reduction of compound **5** by Pd/C and hydrazine. Finally, *N*-methylation of **M1** acquired **M2**. Furthermore, compound **3** was coupled with 4-cyanobenzaldehyde to get compound **6**.

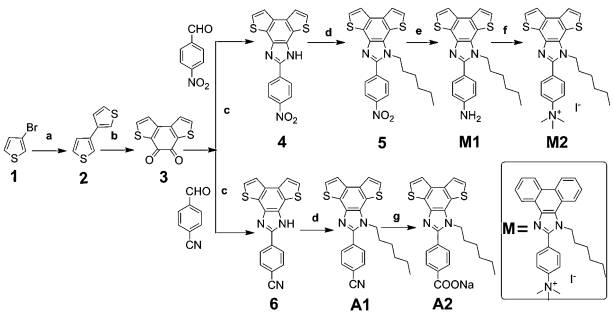

Scheme 1 *Reagents and conditions*: (a) *n*-BuLi, THF, −78 °C to −60 °C, $CuCl_2$, −60 °C to rt, 18 h, 77.9%; (b) CO_2Cl_2, 1,2-DCE, 90 °C, 4 days, 64.65%; (c) NH_4OAc, AcOH, 100 °C, overnight; (d) 1-iodohexane, K_2CO_3, DMF, 95 °C, overnight, (**5** = 80.4%, **A1** = 82.4%); (e) Pd/C, NH_2–NH_2·H_2O, reflux, 4 h, 89.9%; (f) iodomethane, THF, reflux, 72 h, 61.3%; (g) aq. NaOH, EtOH, 2 h, 94%.

Department of Materials Science and Engineering, National Chiao Tung University, Hsinchu 30049, Taiwan, ROC. E-mail: linhc@mail.nctu.edu.tw

† Electronic supplementary information (ESI) available. See DOI: 10.1039/c2cc31131c

Table 1 Photophysical properties of **M1**, **M2**, **A1** and **A2**

Compound	Φ^a	Fluorescence response[b] to Pb^{2+}	Recovery by S^{2-}	τ^c/ns
M1	0.42	Turn off (1.8-fold)	No	1.85
M2	0.04	Turn on (12-fold)	Yes	0.62
A1	0.16	Turn on (5.2-fold)	Yes	0.98
A2	0.26	Turn off (10-fold)	No	1.57

[a] Quantum yields of **M1**, **M2**, **A2** (in DMSO) and **A1** (in THF), 9–10 DPA in THF as a standard (Φ = 0.9). [b] **M1**, **M2**, **A2** (in DMSO/H_2O = 1/1) and **A1** (in THF/H_2O = 1/1). [c] Fluorescence lifetimes.

N-Alkylation of compound **7** afforded **A1**. Further hydrolysis of **A1** by aqueous sodium hydroxide yielded **A2**. According to Scheme S1 (ESI†), a phenanthrene-benzo-imidazole analogue **M** without a 'S' linkage was synthesized to compare its sensitivity with **M2** (with a 'S' linkage).

As shown in Table 1, the quantum yields of **M1**, **M2**, **A1** and **A2** are compared. A strong ICT occurred in **M2** due to the further electron transfer (ET) *via* the negative inductive effect caused by the electron withdrawing quaternary ammonium group, thus reducing the quantum yield of **M2**. Unlike **M2**, backward ET took place in **M1** due to the positive mesomeric effect caused by the lone-pair of electrons on the electron-donating NH_2 group and thus the ICT effect was minimized.[5c] This in turn increased the quantum yield of **M1** (0.42) significantly, compared with **M2** (0.04). The electron cloud shifting can be further explained by the computational analysis illustrated in Fig. S1 (ESI†). Furthermore, the ICT effects were moderate in the case of **A1** and **A2**. The COONa group in **A2** made it a weaker electron-withdrawing group than the cyanide group in **A1** due to the delocalization of electrons in the acetate group. Thus, ICT was more prominent in **A1** than **A2**. As a result, the quantum yield of **A2** (0.26) was higher than **A1** (0.16). The values of fluorescence lifetime (τ) for all compounds obtained from time-resolved fluorescence spectroscopy followed the trend **M1** > **A2** > **A1** > **M2** (see Table 1), which is similar to the trend of the quantum yields. Thus, both fluorescence quantum yields and lifetimes are dependent on the intramolecular ICT occurring in the compounds.

Aqueous solutions of various metal ions such as Na^+, K^+, Mg^{2+}, Ca^{2+}, Ba^{2+}, Ag^+, Co^{2+}, Ni^{2+}, Zn^{2+}, Cu^{2+}, Fe^{2+}, Pb^{2+} and Hg^{2+} were added to the stock solutions of **M2** and **A2**. Their effects on fluorescence signals of **M2** and **A2** (for both single- and dual-metal systems) are depicted in Fig. S3 and S4 (ESI†), respectively. Trivial fluorescent changes were observed in **M2** as other metal ions (Na^+, K^+, Mg^{2+}, Ca^{2+}, Ba^{2+}, Co^{2+}, Ni^{2+}, Zn^{2+}, Cu^{2+}, Fe^{2+} and Hg^{2+}) were added, while a noteworthy enhancement of fluorescence intensity (*ca.* 12-fold) in **M2** was observed in the presence of Pb^{2+} (Fig. 2a). Whereas, **A2** showed a quenching of fluorescence (*ca.* 10-fold) in the presence of Pb^{2+} (Fig. 2b). In the case of **M2**, the ICT effect was further enhanced by the ET effect due to a strong electron-withdrawing quaternary ammonium salt group which in turn minimized the quantum yield of **M2**. Furthermore, upon the addition of Pb^{2+}, both obstruction of ICT and chelation-induced fluorescence enhanced the fluorescence intensity of **M2** (chelation enhanced fluorescence factor, CHEF = 12),[4d] and two new peaks at 403 and 451 nm appeared consequently. ^{1}H NMR titrations with 0–1 equiv.

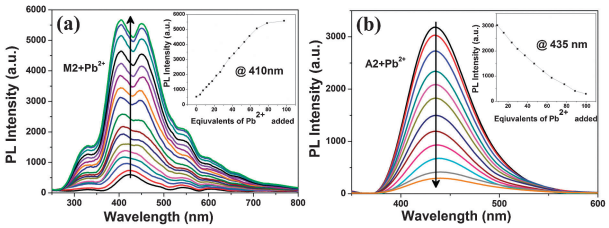

Fig. 2 Fluorescence spectral changes of (a) **M2** (1.4×10^{-5} M) in DMSO/H_2O (1 : 1) (λ_{ex} = 240 nm) and (b) **A2** (1.4×10^{-5} M) in DMSO/H_2O (1 : 1) (λ_{ex} = 265 nm) upon titration of Pb^{2+} (0–1.5×10^{-3} M). Insets show PL spectral responses of (a) **M2** and (b) **A2** as a function of Pb^{2+}.

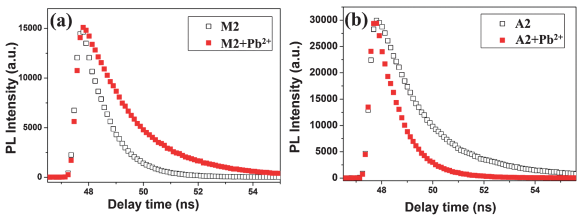

Fig. 3 (a) Time-resolved fluorescence spectra of **M2** (empty circle), and **M2** + Pb^{2+} (solid circle); (b) **A2** (empty square) and **A2** + Pb^{2+} (solid square).

of Pb^{2+} showed significant upfield shifts of peaks corresponding to **M2** (Fig. S5, ESI†). A Job's plot for **M2** by taking the variation of the absorption at 406 nm as a function of [Pb^{2+}]/[**M2**] showed 1 : 1 stoichiometry and the detection limit was obtained as 9.48 μM (Fig. S7, ESI†). Again, based on the time-resolved fluorescence spectra (Fig. 3a), the fluorescence lifetime of **M2** (0.62 ns) was elevated to 1.86 ns upon the addition of Pb^{2+}, which supports the turn-on mechanism. For model compound **M** (where the binding site is only the 'N' atom on the imidazole ring), the ^{1}H NMR and PL titrations did not show any significant changes even at higher concentrations of Pb^{2+} (Fig. S8a and b, ESI†). Thus, it may be concluded that the coordination of Pb^{2+} with both 'S' and 'N' atoms occurred in the dithieno-benzo-imidazole moiety of **M2**, which was the key binding site causing chelation-induced fluorescence enhancement.

However, the CHEF values could be amended by the effective ICT in molecules due to their various substituents. For instance, the ICT effect on **A2** was enhanced owing to the auxiliary electron withdrawing by the COONa group. Thus, upon complexation of Pb^{2+} with **A2**, the fluorescence was expected to be enhanced due to the obstruction of original ICT. Surprisingly, the fluorescence intensity was quenched upon the addition of Pb^{2+} (Fig. 4), which might be attributed to the binding of the metal ions to the COO^- groups. Thus the quencher induced aggregation plays a major role while competing with obstruction of ICT causing quenching of fluorescence. A Stern–Volmer plot for the fluorescence quenching of **A2** indicated that the binding constant of Pb^{2+} for **A2** would decrease upon increasing the temperature which indicated the static quenching mechanism (Fig. S9, ESI†).[6] Furthermore, from Fig. 3b, fluorescence lifetime of **A2** (1.57 ns) decayed to 0.81 ns upon the addition of Pb^{2+}, which was a further evidence for the above-mentioned quenching mechanism.

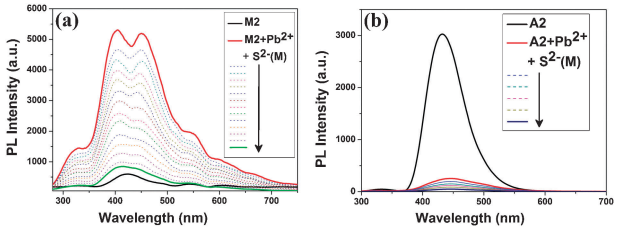

Fig. 4 Fluorescence recovery responses of **M2**–Pb and **A2**–Pb upon titration with 0–0.1 equiv. of S^{2-} (*i.e.*, 0–1.4 × 10^{-6} M) w.r.t. the concentration of **M2**/**A2** (1.4 × 10^{-5} M) (**M2**: λ_{ex} = 240 nm; **A2**: λ_{ex} = 265 nm).

As shown in Table 1 and Fig. S10(a) (ESI†), **A1** showed a turn-on response during sensing of Pb^{2+} similar to **M2**. However, the sensitivity of **A1** (CHEF = 5.2) was lower than that of **M2** (CHEF = 12). This is due to a stronger electron withdrawing effect of the $N^{+}Me_3$ group than CN^{-} causing less favourable ICT in **A1** than **M2**.

Upon complexation of Pb^{2+} with **M1**, the fluorescence intensity was quenched. This can be attributed to the amine group coordinated with the Pb^{2+} ions to cause further electron-withdrawal and thus to quench the fluorescence. Binding of the amine group with metal ions was confirmed by proton NMR titrations (Fig. S11, ESI†). Upon the addition of 10 equiv. of Pb^{2+}, the amine peak at 5.6 ppm completely disappeared. Peaks at 6.72, 7.48, 7.75 and 7.85 ppm in **M1** were shifted to 6.78, 7.55, 7.73 and 7.91 ppm, respectively. Similar to **A2**, upon binding to Pb^{2+}, although ICT was obstructed for **M1**, the quencher-induced aggregation played a major role in causing the fluorescence quenching.

The reversibility of PL for **M2** upon binding to Pb^{2+} was investigated by further addition of different anions, for example Cl^{-}, HCO_3^{-}, HSO_3^{-}, HSO_4^{-}, I^{-}, NO_3^{-}, OH^{-}, PO_4^{3-}, $S_2O_3^{2-}$, SCN^{-} and S^{2-} (Fig. S12, ESI†). Among all these anions, the enhanced PL of the **M2**–Pb complex was mainly annihilated upon the addition of a diminutive amount of S^{2-} (0.1 equiv. w.r.t. the concentration of **M2**). A similar result has been obtained for **A1**–Pb complex upon the addition of S^{2-}. Fluorescence titrations, by the addition of successive aliquots of S^{2-} to the solutions of **M2**–Pb and **A1**–Pb, are illustrated in Fig. 4a and Fig. S13a (ESI†), respectively. To confirm the sensitivity of S^{2-} towards **M2**–Pb and **A1**–Pb complexes, fluorescence signal responses of solo **M2** and **A1** towards S^{2-} in the absence of Pb^{2+} were obtained. As shown in Fig. S14a and b (ESI†), very irrelevant changes in the fluorescence of **M2** and **A1** were observed upon the addition of even higher concentrations of S^{2-} (10 equiv. w.r.t. stock solutions of **M2** and **A1**). This experiment confirmed the sensitivity of S^{2-} towards Pb^{2+} only in their metal–ligand complex state. Similarly, the effects of S^{2-} on **M1**–Pb and **A2**–Pb were tested as depicted in Fig. S13 (b) (ESI†), and Fig. 4(b), respectively. It was found that the fluorescence of the mixtures was further quenched upon the addition of S^{2-}. This can be attributed to the stronger binding of the NH_2 (in **M1**) and COO^{-} groups (in **A2**) to metal ions, which could not be cleaved by S^{2-}. The ICT was restored (in **M1**/**A2**) due to the breakage of imidazole 'N' and 'S' linkages with Pb^{2+}. Moreover, the additional enhancement of ICT, due to the auxiliary binding of metal ions to amine/COONa, caused sheer quenching of fluorescence.

Again we observed that compound **4** showed the best colorimetric and ratiometric sensing ability with F^{-} *via* changing the color of the solution from light yellow to dark pink and shifting of absorption maxima up to 85 nm (from 410 to 495 nm) upon addition of 1 equiv. of F^{-} ions to **4** (Fig. S15, ESI†).

In conclusion, two novel dithieno-benzo-imidazole-based compounds **M2** and **A2** showed remarkable sensitivity towards Pb^{2+} over the other metal ions. In the case of **M2**, the fluorescence was almost 12-fold enhanced. However, the fluorescence of **A2** was quenched almost 10-fold upon titration with Pb^{2+}. Model compound phenanthrene-benzo-imidazole-based **M** has almost no momentous effects during sensing of Pb^{2+}, which indicated the unique sensitivity of dithieno-benzo-imidazole-based **M2** and **A2** towards Pb^{2+} *via* chelation with 'S' and 'N' atoms. The quantum yields and fluorescence lifetime values followed the trend **M1** > **A2** > **A1** > **M2**, which was in consistence with their intramolecular ICT fashion. In the case of **M2** and **A1**, the obstruction of ICT induced the enhancements of fluorescence owing to the binding of a thieno-imidazole unit to Pb^{2+}. However, the quencher-induced aggregation played a major role in the fluorescence quenching for **A2** and **M1** due to the auxiliary binding of NH_2 and COONa with Pb^{2+}. Compared with other anions, trace amounts of S^{2-} induced reversible binding effects of Pb^{2+} with both **M2** and **A1**. Nevertheless, the reversible binding effects of Pb^{2+} by adding S^{2-} were not observed for **M1** and **A2** due to stronger binding of Pb^{2+} with NH_2 and COONa groups, respectively.

The financial support of this project is provided by the National Science Council of Taiwan (ROC) through NSC 99-2113-M-009-006-MY2 and National Chiao Tung University through 97W807.

Notes and references

1 (*a*) F. Teixidor, M. A. Flores, L. Escriche, C. Viñas and J. Casabó, *Chem. Commun.*, 1994, 963; (*b*) S. Chung, W. Kim, S. B. Park, I. Yoon, S. S. Lee and D. D. Sung, *Chem. Commun.*, 1997, 965; (*c*) K. Kimura, S. Yajima, K. Tatsumi, M. Yokoyama and M. Oue, *Anal. Chem.*, 2000, **72**, 5290; (*d*) A. Ceresa, A. Radu, S. Peper, E. Bakker and E. Pretsch, *Anal. Chem.*, 2002, **74**, 4027.

2 (*a*) A. P. de Silva, H. Q. N. Gunaratne, T. Gunnlaugsson, A. J. M. Huxley, C. P. McCoy, J. T. Rademacher and T. E. Rice, *Chem. Rev.*, 1997, **97**, 1515; (*b*) V. Amendola, L. Fabbrizzi, M. Licchelli, C. Mangano, P. Pallavicini, L. Parodi and A. Poggi, *Coord. Chem. Rev.*, 1999, **190–192**, 649; (*c*) L. Prodi, F. Bolletta, M. Montalti and N. Zaccheroni, *Coord. Chem. Rev.*, 2000, **205**, 59; (*d*) Q. Zhao, F. Y. Li and C. H. Huang, *Chem. Soc. Rev.*, 2010, **39**, 3007; (*e*) B. Valeur and I. Leray, *Coord. Chem. Rev.*, 2000, **205**, 3; (*f*) A. K. Dwivedi, G. Saikia and P. K. Iyer, *J. Mater. Chem.*, 2011, **21**, 2502; (*g*) B. Chetia and P. K. Iyer, *Tetrahedron Lett.*, 2008, **49**, 94.

3 J. S. Liu-Fu, *Lead Poisoning: A Century of Discovery and Rediscovery*, in *Human Lead Exposure*, ed. H. L. Needleman, Lewis Publishing, Boca Raton, FL, 1992.

4 (*a*) R. Zhou, B. Li, N. Wu, G. Gao, J. You and J. Lan, *Chem. Commun.*, 2011, **47**, 6668; (*b*) M. Alfonso, A. T'arraga and P. Molina, *Dalton Trans.*, 2010, **39**, 8637; (*c*) M. Alfonso, A. Espinosa, A. T'arraga and P. Molina, *Org. Lett.*, 2011, **13**, 2078; (*d*) M. Alfonso, A. T'arraga and P. Molina, *J. Org. Chem.*, 2011, **76**, 939; (*e*) Z.-Q. Hu, C.-S. Lin, X.-M. Wang, L. Ding, C.-L. Cui, S.-F. Liu and H. Y. Lu, *Chem. Commun.*, 2010, **46**, 3765; (*f*) X.-L. Ni, S. Wang, X. Zeng, Z. Tao and T. Yamato, *Org. Lett.*, 2011, **13**, 552.

5 (*a*) C. Qin, W. Y. Wong and L. Wang, *Macromolecules*, 2011, **44**, 483; (*b*) C. Qin, Y. Cheng, L. Wang, X. Jing and F. Wang, *Macromolecules*, 2008, **41**, 7798; (*c*) M. Dekhtyar, W. Rettig and W. Weigel, *Chem. Phys.*, 2008, **344**, 237.

6 S. Sirilaksanapong, M. Sukwattanasinitt and P. Rashatasakhon, *Chem. Commun.*, 2012, **48**, 293.

